Synergistic Approach for Computational Analysis of Geomagnetically Induced Currents in Power Grids

Adebola Oke[1], Pablo Gomez[2]
Electrical and Computer Engineering,
Western Michigan University,
Kalamazoo, MI 49008, USA
[1]adebolaenoch.oke@wmich.edu,
[2]pablo.gomez@wmich.edu

***Abstract*— Geomagnetically induced currents (GICs) have the potential to be highly disruptive to regular power grid operations. Despite the study of geomagnetic disturbances (GMDs) since the 1940s, comprehensive methods for accurate and precise analysis of their impact, especially in individual grid components, remain limited. This paper describes a method based on the synergistic use of different computational tools for detailed simulation of GMDs in power grids. The proposed methodology allows the effective integration between three main aspects required for accurate determination of GICs and their effects on power systems: (1) location-specific estimation of Earth's magnetic fields at ground level, (2) detailed physics-based ground impedance modeling considering specific geological environment, and (3) power grid modeling considering detailed network and grounding topology. The goal is to generate an end-to-end methodology for GIC calculation in power grids from the magnetic field environment during a geomagnetic event, the soil conductivity profile at the site of interest, and the grid topology data. The resulting methodology was evaluated by means of a sample case that utilizes magnetic field data from an actual event.**

***Index Terms*—GIC, GMD, Geomagnetically Induced Currents, Transmission Lines**

I. Introduction

Geomagnetic storms are a type of space weather event in which the Earth's magnetic field interacts with magnetic solar material [1], [2]. Variations in the Earth's magnetic field produced by this interaction result in electric field variations according to Faraday's law of induction. Furthermore, these electric fields give rise to low-frequency currents, known as *geomagnetically induced currents (GIC)* flowing along conducting paths of large extension, such as power transmission lines, pipelines, and railways [2]. In the case of transmission lines, GIC occurrence and impact has become substantially more significant over the last decades with the exponential growth in electric grids, as well as the trend towards the use of higher transmission voltages and lower line resistances to reduce transmission losses over long distances, which results in electric power systems that are more susceptible to GIC effects. GIC can affect various power components, such as transformers, generators, protection devices, grid communication systems, etc. Depending on the severity and duration of a geomagnetic event, the effects of GIC can range from minor fluctuations in the power grid to malfunctioning of protection devices, damage of power apparatus, and even complete power outages [3].

Power grid issues due to GIC phenomena have been reported for many decades. One of the most significant GIC cases was reported during an extreme geomagnetic disturbance in 1989, which resulted in the collapse of the Hydro-Quebec grid in Canada [4], as well as transformer damage in the US [5]. Fourteen more cases were reported between 1989 and 1992 in North America, where GIC produced maloperation of protection devices [6]. Numerous additional instances of GIC effects on the grid have been reported around the world [3]. At the same time, there has been considerable growth in high voltage power grids and smart grid technologies. Therefore, there is a profound need to investigate the GICs impact on these modern power systems [3].

Building resilience against GIC in power grids requires tools for effective prediction and evaluation of this phenomenon [7], so that appropriate countermeasures can be incorporated during design, testing and operation. Experimental and computational tools have been developed for this purpose. Field measurement of GIC in power lines using transducers at transformers neutrals can be a reliable monitoring strategy, but it can also be cost prohibitive considering the size and complexity of modern grids. Alternatively, computational modeling and simulation tools can be applied to predict and evaluate GIC conditions and their impact on grid operation [8]. Effective modeling of GIC phenomenon involves three main aspects: (1) estimation of magnetic field components at ground level, (2) ground modeling for calculation of electric field from magnetic field, and (3) power grid and grounding system modeling [9]. The appropriate combination of these aspects is an area under substantial research and development [3], [9].

Several commercial power system analysis tools have incorporated GIC studies [2], [10]. These tools allow detailed electric grid models, but the sources of GIC are commonly

2023 North American Power Symposium (NAPS) | 979-8-3503-1509-7/23/$31.00 ©2023 IEEE | DOI: 10.1109/NAPS58826.2023.10318742

Authorized licensed use limited to: WESTERN MICHIGAN UNIVERSITY. Downloaded on February 05,2024 at 14:37:17 UTC from IEEE Xplore. Restrictions apply.

simplified by *dc* sources and the ground modeling effect is not considered in detail. This can have a detrimental effect on the accurate prediction of GIC conditions on grid components. Similar limitations can be found in existing GIC studies in power transformers, where the device is typically modeled in full detail, but the impact of GIC is simplified as a *dc* bias (see for instance [11]-[14]). This can result in an inaccurate prediction of abnormal transformer conditions, which range from thermal stress to grid voltage collapse due to saturation [15]. Other studies have focused on providing accurate ground models [8], [16], a crucial step to link magnetic field estimation at ground level with the evaluation of GIC effect on power systems. Since the focus of these studies is on the detailed evaluation of ground impedance, they tend to simplify the grid model and/or geomagnetic field estimation.

In this paper we propose a methodology based on the synergistic combination of modeling and simulation tools for the prediction and evaluation of GIC in electric power systems. The proposed methodology allows the effective integration between the three main aspects required for accurate determination of GIC and their effects on power systems: (1) location-specific estimation of Earth's magnetic fields at ground level, (2) detailed physics-based ground impedance modeling considering specific geological environment, and (3) power grid modeling considering fully detailed network and grounding topology.

II. Methodology

The proposed methodology, depicted in Fig. 1, involves the following main steps:

STEP 1: The main input of the modeling approach is the measurement of the Earth's magnetic field in the time domain for an appropriate time window and a specific location. This information is retrieved from the International Real-Time Magnetic Observatory Network (intermagnet.org) [17].

STEP 2: The magnetic field components obtained in the previous step are used as inputs for a finite element analysis (FEA)-based ground impedance model. The software used for this purpose is COMSOL Multiphysics. The output of this model is the calculation of horizontal electric field through the soil model.

STEP 3: This step involves building and solving a conductance-based model of the grid under test as outlined in the proposed methodology. As described in [18], the system to be solved has the form:

$$\mathbf{V}(t) = \mathbf{G} \quad \mathbf{J}(t) \tag{1}$$

where $\mathbf{V}(t)$ is a column vector containing the nodal voltages of the system as a function of time; $\mathbf{G}$ is the conductance matrix of the system including conductances of substations, transmission lines, transformers, and grounding system; and $\mathbf{J}(t)$ is a column vector of time-varying injection currents obtained from the Norton equivalent of the induced voltages representing the line integration of the electric field obtained in the previous step. This integration requires the location of each substation between lines to define the corresponding integration path. Eq. (1) is solved for the nodal voltages vector $\mathbf{V}(t)$.

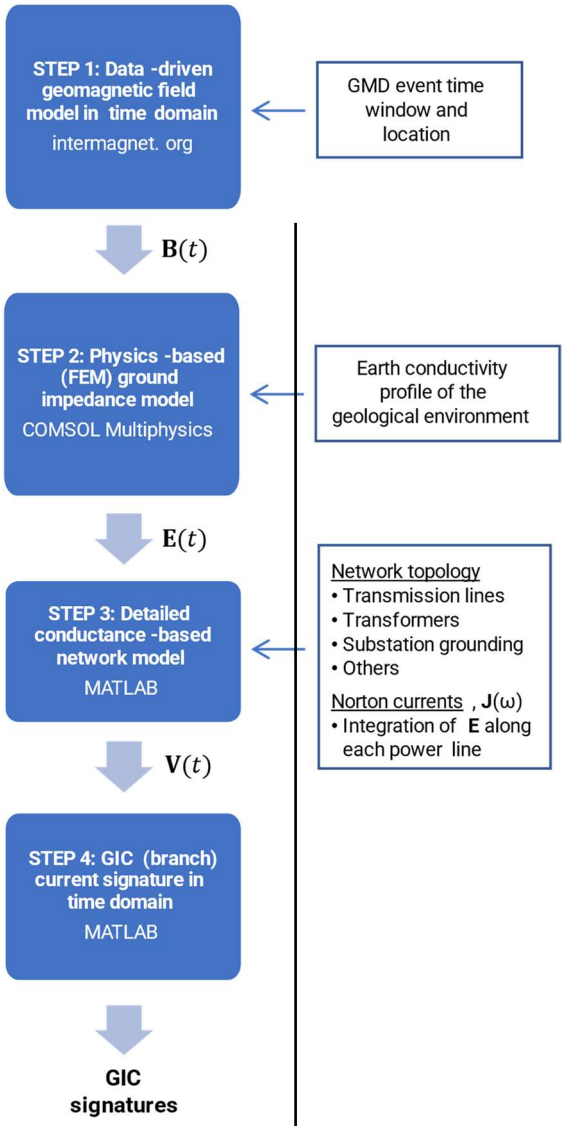

Fig. 1 Proposed methodology for GIC calculation.

STEP 4: This step involves the calculation of geomagnetically induced currents as time domain signatures. These include branch currents along the lines and currents to ground from each node. Branch currents in the lines are calculated as follows:

$$I_{i,k}(t) = J_i(t) - J_k(t) + G_{i,k}\,[V_i(t) - V_k(t)] \tag{2}$$

where $I_{i,k}$ is the geomagnetically induced current between nodes i and k of the system, J_i, J_k, V_i and V_k are the injection currents and nodal voltages at nodes i and k, and $G_{i,k}$ is the equivalent conductance connected between nodes i and k. The currents to ground from each node are calculated as

$$I_{i,g}(t) = G_{i,g}\,V_i(t) \tag{3}$$

where $I_{i,g}(t)$ is the geomagnetically induced current between node i and ground, $V_i(t)$ is the voltage at node i, and $G_{i,g}$ is the equivalent admittance connected between node i and ground.

Authorized licensed use limited to: WESTERN MICHIGAN UNIVERSITY. Downloaded on February 05,2024 at 14:37:17 UTC from IEEE Xplore. Restrictions apply.

III. Small Synthetic Sample Case

A reference case with detailed results available was used for initial assessment of the proposed procedure. The test case utilized is described in [19], [20]. This initial comparison aims to provide confidence in the calculation of GICs flowing through each grid component.

This initial test corresponds to a synthetic grid with assumed resistive values. The grid is induced by a predetermined and constant electric field of 1 V/km in all directional components to simplify the GIC calculation. GMDs are assumed to induce perfectly tangential magnetic fields and corresponding electric fields along the transmission lines and other components. It should be noted that, since this synthetic test case assumes an induced uniform electric field of 1 V/km along the line, an input vector field from COMSOL is not required.

With the test case as described, a conductance matrix is determined from the topological grid information and the parameters provided in order to compute the bus voltages and induced GICs. The sample grid is illustrated by the single-line conductance diagram in Fig. 2, with all numerical values, such as resistances/conductances and transmission line lengths, retained from [20]. This single-line diagram includes the conductance components to appropriately integrate the substation neutral buses, grounding resistances, generators, and autotransformers.

In Fig. 2, TL1 And TL2 represent transmission lines 1 and 2 (each with a length of 150 km), while Tx represents the autotransformer connected between the lines.The system nodes are indicated in red, the conductances are shown in blue, and their calculation for each component is shown in green. For instance:

- the resistance of transmission line 1 is 3 Ω/phase, so its equivalent conductance is calculated as 3/3 Ω = 1 S;
- the resistance of the generator at substation A is 0.15 Ω/phase, so its conductance is 3/0.15 Ω = 20 S; and
- the grounding resistance of substantion A is 0.20 Ω, therefore its equivalent conductance is 1/0.20 Ω = 5 S.

Similar calculations are performed for other power and grounding components of the grid. Table I shows the resulting conductance matrix.

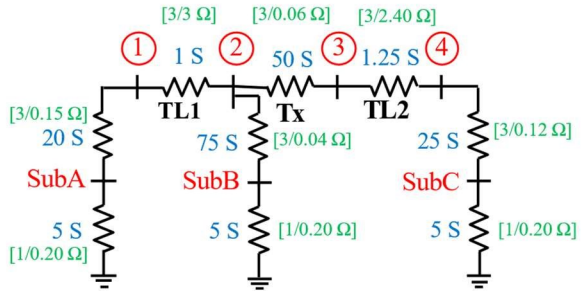

Fig. 2 Equivalent conductance circuit of test case

TABLE I. Conductance Matrix of Synthetic System (in Siemens)

	SubA	SubB	SubC	1	2	3	4
SubA	25	0	0	-20	0	0	0
SubB	0	80	0	0	-75	0	0
SubC	0	0	30	0	0	0	-25
1	-20	0	0	21	-1	0	0
2	0	-75	0	-1	126	-50	0
3	0	0	0	0	-50	51.25	-1.25
4	0	0	-25	0	0	-1.25	26.25

Using this conductance matrix, the algorithm generates the corresponding GICs. This includes GIC flow in each transmission line, autotransformer winding, substation generator, and grounding resistances. Since transmission line sensitivity to GIC is the main focus of the study in [20], the results for the other grid components were not provided. The results of GIC in the transmission lines were approximately 40.9 A and 46.1 A, respectively, matching the values calculated in [20]. Table II lists the GIC flow calculated in all system components. From Table II, we can see that the algorithm is able to calculate the induced GIC in all system components, as well as the appropriate direction, determined by the current sign.

TABLE II. Induced GICs

Grid Component	Induced GIC (A)
Transmission line 1	40.8919
Transmission line 2	46.1180
SubA ground resistance	-40.8919
SubB ground resistance	-5.2261
SubC ground resistance	46.1180
Autotransformer common windings	5.2261
Autotransformer series windings	46.1180

IV. Time-Dependent Case Using Real Magnetic Data

After verifying the correct performance of the methodology, the following test case considers a more realistic scenario to assess the entire procedure, including the FEA-based calculation of time-dependent electric field components from location-specific soil profile and measurements of magnetic field data. This test aims to confirm the algorithm's ability to carry out time dependent GIC calculations for all interconnected grid components using the electric field vector obtained from COMSOL.

Reliable GIC data was required for the quantitative assessment of the results of this test, which was obtained from a comparative study of peak electric fields and GICs in the Pacific Northwest region [21]. This study made use of three-dimensional magnetic field data from the Intermagnet Newport observatory and a CO1 soil conductivity profile from [22], which were applied in calculating the peak electric field and peak GIC induced in the electric grid for this region during the 2003 Halloween GMD event. The *XYZ* components of the Newport magnetic field data are extracted using a Python-based mag-field plotter tool called MagPy [23], which generates location-specific data from magnetic field stations around the world. To exemplify the results from MagPy, Fig 3 shows the *x*-axis data plotted by this tool. Fig. 4 shows the FEM-based soil model developed in COMSOL. The *x*-component of the

Authorized licensed use limited to: WESTERN MICHIGAN UNIVERSITY. Downloaded on February 05,2024 at 14:37:17 UTC from IEEE Xplore. Restrictions apply.

magnetic field is applied as input to this model for the calculation of the equivalent horizontal (*y*-component) electric field. The calculation of the electric field from the magnetic field is done for every equivalent two axes, given that the COMSOL soil model used is two dimensional. The soil conductivity profile by layers, as set up in COMSOL, is provided in Table 3. The relative permittivity and permeability values of the entire soil model are both defined as 1 (equal to those of free space), assuming no magnetic or dielectric properties of the soil.

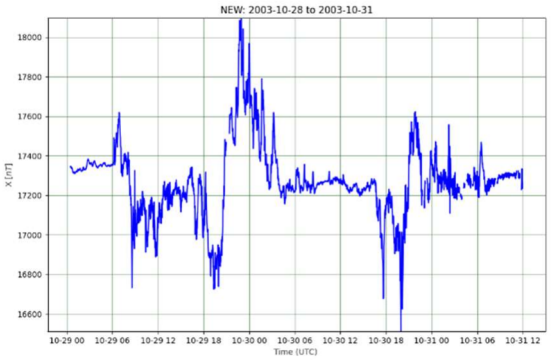

Fig. 3 *X*-component of magnetic field from Newport Intermagnet observatory for the 2003 Halloween event, as plotted by MagPy.

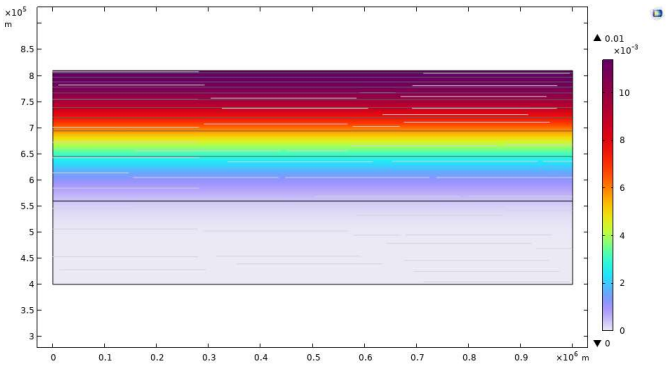

Fig. 4 Layered soil model for FEM-based calculation of electric field (V/m) generated over the region of interest during the 2003 Halloween event.

TABLE III. SOIL CONDUCTIVITY PROFILE

Layer	Width (km)	Depth (km)	Conductivity (S/m)
1	1000	0-200	1/361
2	1000	200 – 400	1/10

Fig. 5 shows the electric field calculated from COMSOL using the Newport Intermagnet data. This data is used to calculate the corresponding Norton equivalents included in the netlist, which are introduced into the network analysis algorithm along with the grid topology and parameters data.

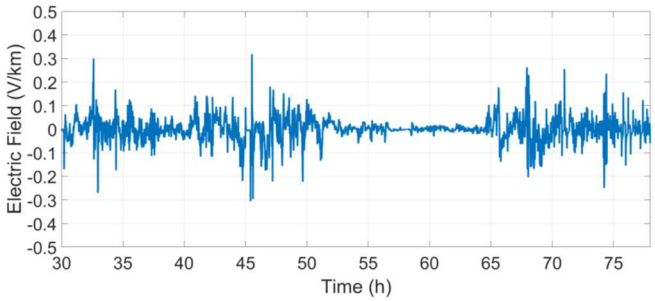

Fig. 5 Electric field (V/km) generated at the region's surface (transmission line level) during the Halloween event as calculated by COMSOL.

The study in [21] made use of a representative grid with 13 nodes corresponding to substation locations within the analysis footprint and spanning the entire region. For our study, the representative grid from the ideal case in Section III with three substations and two lines is retained, since we did not have access to the protected BPA utility data from [21]. However, this should still provide a reasonable analysis taking into account that GMDs are continent wide events that are better studied closer to the transformers (areas) of interest [19], [20]. Therefore, since just one of the subregions' soil conductivity profiles is employed in COMSOL at a time, the small example grid model from [20] can produce similar GIC profiles to the ones calculated in a larger representative grid.

Fig. 6 shows the calculated GIC along the two 150 km transmission lines from the example grid when subjected to the same electric field induced by the 2003 Halloween event GMDs. The blue waveform corresponds to the GIC induced in transmission line 1, while the orange waveform corresponds to the GIC along transmission line 2. The GIC profiles in both of these lines are consistent with the range of peak values of the thirteen representative nodes from [21]. As observed in Figs. 5 and 6, the time varying electric field data generated by COMSOL provide detailed insights into the time domain behavior of the GIC along the lines, highlighting time periods where extreme geomagnetic activity may have caused GICs to spike beyond the calculated peaks in [21].

Fig. 7 shows the results of induced GIC waveforms in all grid components for the 2003 Halloween event. These results demonstrate the algorithm's ability to estimate the induced GICs in individual power grid components over time. It can be noticed that the oscillatory behavior of the electric field plot from Fig. 5 matches that of the GIC plots, with the time periods of high electric field spikes correlating with the highest GICs induced in the system. Simple nodal analysis at any node can also be carried out correlating instantaneous GIC values of these individual components to confirm the accurate simulation of GIC flow in the grid. This analysis therefore confirms that the algorithm, at every instant in time, follows Kirchhoff's law of currents.

Authorized licensed use limited to: WESTERN MICHIGAN UNIVERSITY. Downloaded on February 05,2024 at 14:37:17 UTC from IEEE Xplore. Restrictions apply.

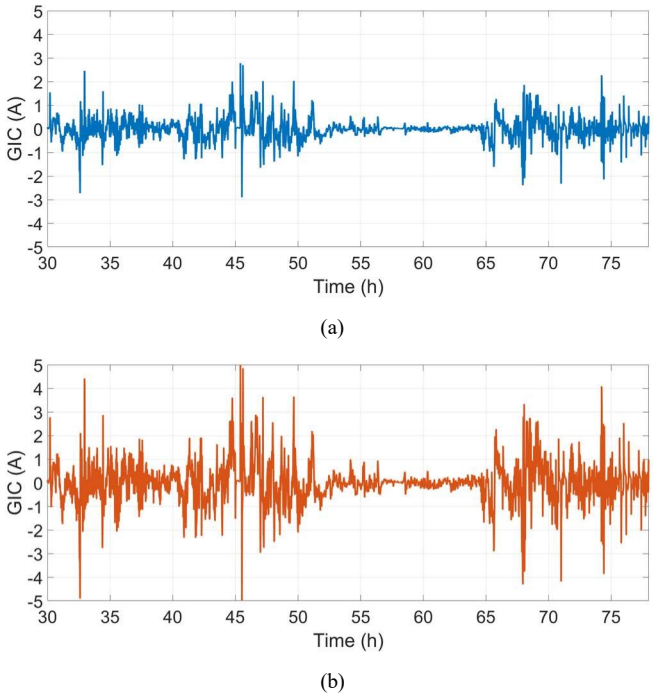

Fig. 6 GIC induced in transmission lines 1 and 2 over the CO1 region using the 2003 GMDs.

V. Conclusions

Previous research concluded that the primary limitations of GIC estimation lie in how well the combination of available input data represent the actual magnetic variation, the Earth conductivity, and the system characteristics, rather than in the accuracy of the methodology itself [19]. With this in mind, our main goal for this preliminary work has been to provide a methodology to integrate the main software packages (MATLAB, COMSOL and MagPy) as a comprehensive and computationally efficient means to accurately represent and overcome the aforementioned limitations. The proposed methodology helps to overcome the need for compromises such as using peak electric field values for calculations, allowing for more accurate time dependent results, which are paramount to fully estimate electric field response [21]. Accurate 1D, 2D or 3D soil models can be easily integrated into the algorithm to fine-tune the method's resolution and accuracy as long as the data are available. Finally, directional variations in GMDs induced in specific grid components and their unique electrical parameters can be accounted for in a straightforward manner, allowing for accurate multidirectional simulation of GIC flow in individual grid components.

Acknowledgment

Research reported in this publication was supported in part by funding provided by the National Aeronautics and Space Administration (NASA), under award number 80NSSC20M0124, Michigan Space Grant Consortium (MSGC). In addition, the authors thank the Summer of Power Engineering Research Initiation and Training (SPERIT) program at WMU Power Lab, funded through NSF grant #2138408, for supporting this research work.

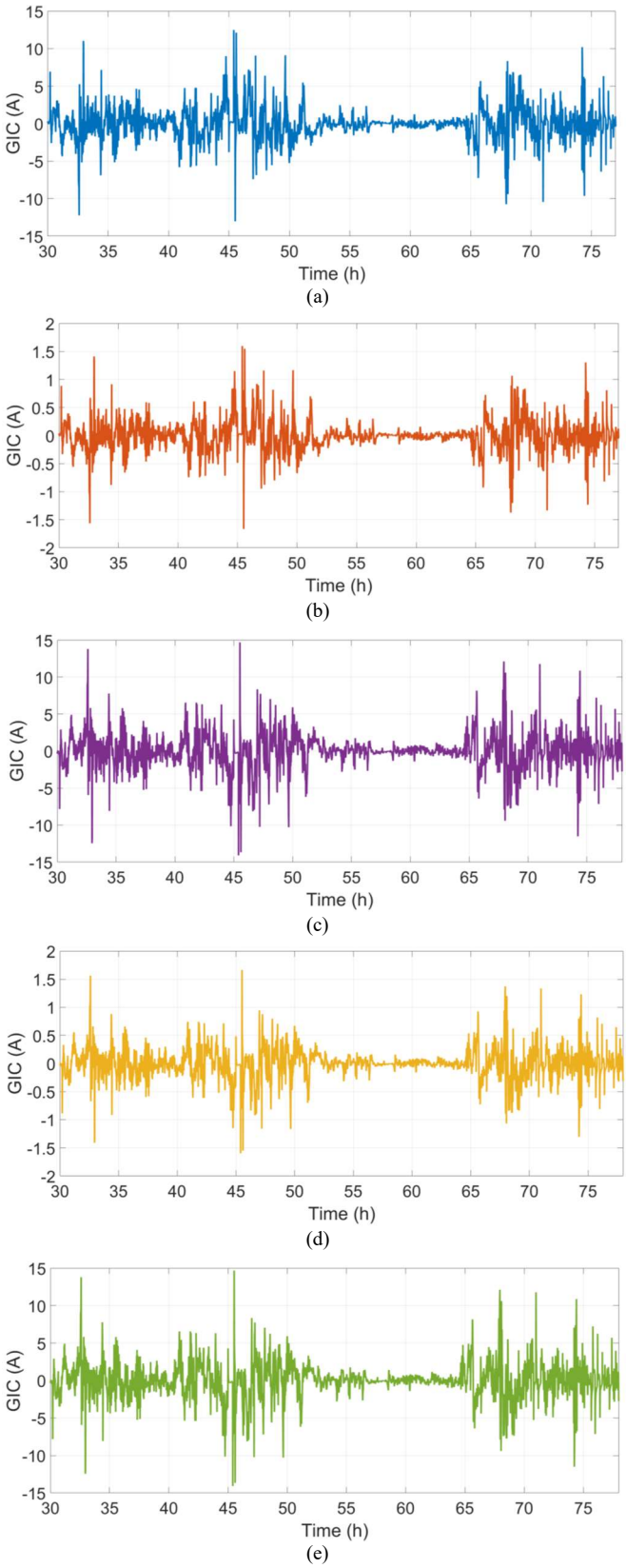

Fig. 7 GIC over the CO1 region using the 2003 Halloween event GMDs: (a) Substation A, (b) Substation B, (c) Substation C, (d) autotransformer common windings, (e) autotransformer series windings.

Authorized licensed use limited to: WESTERN MICHIGAN UNIVERSITY. Downloaded on February 05,2024 at 14:37:17 UTC from IEEE Xplore. Restrictions apply.

REFERENCES

[1] NASA Jet Propulsion Laboratory – California Institute of Technology, "Geomagnetically Induced Currents (GICs)", April 19, 2017. Available online: https://www.jpl.nasa.gov/infographics/geomagnetically-induced-currents-gics

[2] "GIC Quick Start Guide", Power World Corporation, March 2012. Available online: https://www.powerworld.com/files/GICModeling.pdf

[3] V. N. Rajput, D. H. Boteler, N. Rana, M. Saiyed, S. Anjana, M. Shah, "Insight into impact of geomagnetically induced currents on power systems: Overview, challenges and mitigation," *Electric Power Systems Research*, vol. 192, March 2021

[4] S. Guillon, P. Toner, L. Gibson, D. Boteler, "A colorful blackout: the havoc caused by auroral electrojet generated magnetic field variations in 1989," *IEEE Power and Energy Magazine*, vol. 14, no. 6, pp. 59-71, Nov.-Dec. 2016

[5] D. H, Boteler, "A 21st Century View of the March 1989 Magnetic Storm," *Space Weather*, vol. 17, no. 10, pp. 1427-1441, Oct. 2019

[6] B. Bozoki et al., "The effects of GIC on protective relaying," *IEEE Transactions on Power Delivery*, vol. 11, no. 2, pp. 725-739, April 1996

[7] K. S. Shetve, A. B. Birchfield, R. H. Lee, T. J. Overbye and J. L. Gannon, "Impact of 1D vs 3D Earth Conductivity Based Electric Fields on Geomagnetically Induced Currents," *2018 IEEE PES Innovative Smart Grid Technologies Conference Europe*, Sarajevo, Bosnia and Herzegovina, Oct. 2018

[8] E. Matandirotya, "Measurement and Modelling of Geomagnetically Induced Currents (GIC) in Power Lines," Ph.D. Thesis, Cape Peninsula University of Technology, South Africa, July 2016

[9] A. Kelbert "The Role of Global/Regional Earth Conductivity Models in Natural Geomagnetic Hazard Mitigation," *Surveys in Geophysics*, vol. 41, pp. 115–166, 2020

[10] R. Dugan, "Geo-Magnetic Disturbance Analysis of HV and EHV Grids," *Modeling, Simulation, and Optimization for the 21st Century Electric Power Grid*, Lake Geneva, WI, USA, Oct. 2012

[11] A. Rezaei-Zare, "Behavior of Single-Phase Transformers Under Geomagnetically Induced Current Conditions," *IEEE Transactions on Power Delivery*, vol. 29, no. 2, pp. 916-925, April 2014

[12] F. Aboura, O. Touhami, "Effect of the GICs on magnetic saturation of asymmetric three-phase transformer," *IET Electric Power Applications*, vol. 11, no. 7, Aug. 2017

[13] H. K. Chisepo, C. T. Gaunt and L. D. Borrill, "Measurement and FEM analysis of DC/GIC effects on transformer magnetization parameters," *2019 IEEE Milan PowerTech*, Milan, Italy, June 2019

[14] S. Mkhonta, T. T. Murwira, D. T. O. Oyedokun, K. A. Folly and C. T. Gaunt, "Investigation of Transformer Reactive Power and Temperature Increases Under DC," *IEEE PES/IAS PowerAfrica*, Cape Town, South Africa, June 2018

[15] R. S. Girgis and K. B. Vedante, "Impact of GICs on Power Transformers: Overheating is not the real issue.," *IEEE Electrification Magazine*, vol. 3, no. 4, pp. 8-12, Dec. 2015

[16] C. M. Ngwira, A. Pulkkinen, L. A. McKinnell, and P. J. Cilliers, "Improved modelling of geomagnetically induced currents in the South African power networks," *Space Weather*, vol. 6, no. 11, 2008.

[17] International Real-time Magnetic Observatory Network. Available online: https://intermagnet.github.io/

[18] D. Boteler, "Methodology for simulation of geomagnetically induced currents in power systems," *Journal of Space Weather and Space Climate*, vol. 4, no. A21, July 2014

[19] R. Horton, D. Boteler, T. J. Overbye, R. Pirjola and R. C. Dugan, "A Test Case for the Calculation of Geomagnetically Induced Currents," *IEEE Transactions on Power Delivery*, vol. 27, no. 4, pp. 2368-2373, Oct. 2012

[20] T. J. Overbye, K. S. Shetye, T. R. Hutchins, Q. Qiu and J. D. Weber, "Power Grid Sensitivity Analysis of Geomagnetically Induced Currents," in *IEEE Transactions on Power Systems,* vol. 28, no. 4, pp. 4821-4828, Nov. 2013

[21] J. L. Gannon, A. B. Birchfield, K. S. Shetye, and T. J. Overbye, "A comparison of peak electric fields and GICs in the Pacific Northwest using 1-D and 3-D conductivity" *Space Weathe*r vol. 15, no 11 1535–1547. Oct. 2017

[22] P. Fernberg, "One-dimensional earth resistivity models for selected areas of continental United States and Alaska," *EPRI technical update 1026430*, 105-135, 2012

[23] R. Leonhardt, R. Bailey, M. Miklavec, J. Fee, H. Schovanec. *Magpy 1.0.3 Geomagnetic Analysis Tool.* (2022). Available online: https://github.com/geomagpy/magpy

Authorized licensed use limited to: WESTERN MICHIGAN UNIVERSITY. Downloaded on February 05,2024 at 14:37:17 UTC from IEEE Xplore. Restrictions apply.